Introduction

Seismic interferometry (SI) is usually applied to retrieve the impulse response between receiver pairs, turning one of the receivers into a virtual source. In the case of having actual receivers in the subsurface, this method has been applied to successfully redatum the data to a deeper part of the subsurface without an accurate velocity model of the overburden. This type of interferometry is referred as inter-receiver SI. By invoking source-receiver reciprocity, one can also retrieve the impulse response between source pairs, turning one of the sources into a virtual receiver (Curtis et al., 2009). This type of interferometry is referred as inter-source SI. Similarly, with inter-source SI, it is possible to redatum the data into the subsurface without deploying any receivers in the subsurface. This can be of particular interest when one only has noise sources in the subsurface. One such example may be drill-bit noise.

There are different ways to implement seismic interferometry. The typical approach is by crosscorrelation (CC). Although straightforward and robust, it is theoretically only valid in a medium without loss and may suffer from imperfect acquisition geometries. An alternative approach is multi-dimensional deconvolution (MDD), which essentially is an inversion process and has the potential to suppress artifacts due to irregular source distribution and intrinsic loss (Wapenaar et al, 2011).

In a recent abstract, we extend the theory of inter-receiver SI to inter-source SI by MDD for transient subsurface sources (Liu et al., 2013). In a general situation, the method requires the separation of incoming and outgoing waves at source locations, which, in the case of demultipled data, reduces to the separation of the direct and reflected waves. However, such a separation in the data domain may be problematic for non-transient sources. Following the work by Wapenaar and Fokkema (2006) and van der Neut et al. (2010), here we show that for inter-source SI, the separation can also be made by time-windowing in an intermediate crosscorrelation step of the MDD inversion procedure, provided that the noise sources have the same signal signature. This approach opens possibilities for turning noise sources into virtual receivers in the subsurface.

Theory

Starting from Rayleigh's reciprocity theorem of the convolution type (Wapenaar and Fokkema, 2006) and defining two states A and B as shown in Figure 1,

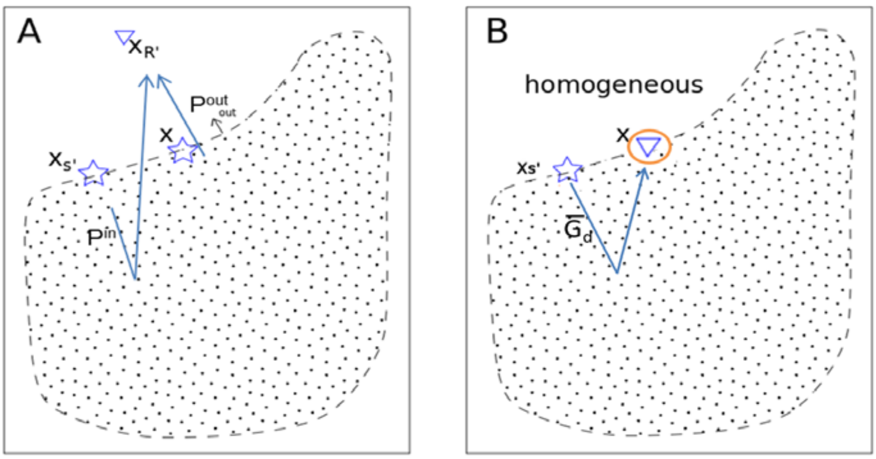

Figure 1 Configurations of state A and B for inter-source SI by MDD. The dotted line describes the boundary enclosing the integral volume. The orange circle denotes the virtual receiver. The star denotes a source and the triangle denotes a receiver.

we derive the basic equation for inter-source SI by MDD with sources in the subsurface as (Liu et al, 2013):

$$P^{in}(\mathbf{x}_{R'} \mid \mathbf{x}_{S'}) = \int P^{out}(\mathbf{x}_{R'} \mid \mathbf{x}) \bar{G}_d^{in}(\mathbf{x} \mid \mathbf{x}_{S'}) d\mathbf{x} \qquad ①$$

The capital letters indicate the frequency domain. It means that the convolution of the pressure field $P^{out}(\mathbf{x}_{R'} \mid \mathbf{x})$ (outgoing from X to $X_{R'}$) and the dipole Green's function $\bar{G}_d^{in}(\mathbf{x} \mid \mathbf{x}_{S'})$ (incoming from $X_{S'}$ to X), summed over all source positions, gives the pressure field $P^{in}(\mathbf{x}_{R'} \mid \mathbf{x}_{S'})$ (incoming from $X_{S'}$ to $X_{R'}$). The dipole Green's function is defined in equation ②. The bar denotes that the retrieved Green's function is defined in state B where the medium outside the source surface is homogeneous.

$$\bar{G}_d^{in}(\mathbf{x} \mid \mathbf{x}_{S'}) = \frac{-2}{j\omega\rho(\mathbf{x})} n_i \partial_i \bar{G}^{in}(\mathbf{x} \mid \mathbf{x}_{S'}) \qquad ②$$

The Least Square inversion of equation ① is equivalent of solving the normal equation (Menke, 1989), with the integral written out explicitly as:

$$\int P^{out*}(\mathbf{x}_{R'} \mid \mathbf{x}') P^{in}(\mathbf{x}_{R'} \mid \mathbf{x}_{S'}) d\mathbf{R} = \int \left[\int P^{out*}(\mathbf{x}_{R'} \mid \mathbf{x}') P^{out}(\mathbf{x}_{R'} \mid \mathbf{x}) d\mathbf{R} \right] \bar{G}_d^{in}(\mathbf{x} \mid \mathbf{x}_{S'}) d\mathbf{x} \qquad ③$$

with $\Gamma(x', x) = \int P^{out*}(\mathbf{x}_{R'} \mid \mathbf{x}') P^{out}(\mathbf{x}_{R'} \mid \mathbf{x}) d\mathbf{R}$, where $*$ denotes the complex conjugate and $\Gamma(x', x)$ is called the point spread function (PSF) (van der Neut et al., 2010; Wapenaar et al., 2011). The solution of the above system of equations, which is the unknown dipole Green’s function between two source positions, can be estimated with a standard Damped Least Squares approach. The notation is switched to the matrix form:

$$\bar{G}_d^{out} = (P^{out\dagger} P^{out} + \varepsilon^2 I)^{-1} P^{out\dagger} P^{in} \qquad ④$$

where $\dagger$ denotes the complex conjugate transpose. In an ideal case where the free-surface multiples and the inter-layer multiples have been removed, P^{out} reduces to the direct wave and P^{in} to the reflected wave. Therefore, the implementation of equation ④ requires the separation of these two wavefields, which poses limitation for non-transient sources. However, writing out $P^{\dagger}P$ with the total field $P = P^{out} + P^{in}$ gives:

$$P^{\dagger}P = P^{out\dagger}P^{out} + P^{out\dagger}P^{in} + P^{in\dagger}P^{out} + P^{in\dagger}P^{in} \qquad ⑤$$

For noise sources, if all sources have the same signature, the integral in the PSF function in equation ③ can be replaced by a spatial ensemble average $\langle \cdot \rangle$ (Wapenaar and Fokkema, 2006), and using the notation where P stands for vectors, we can rewrite equation ④ for noise sources as:

$$\bar{G}_d^{out} = \left(\left\langle P^{out\dagger} P^{out} \right\rangle + \varepsilon^2 I \right)^{-1} \left\langle P^{out\dagger} P^{in} \right\rangle \qquad ⑦$$

Now in the total crosscorrelation panel $\langle P^{\dagger}P \rangle$, one can find the term $\langle P^{out\dagger}P^{out} \rangle$ to have its major contribution around |t|=0 and the term $\langle P^{out\dagger}P^{in} \rangle$ will have its at t>t1, where t1 is the two-way travel time of the first reflector. The last term $\langle P^{in\dagger}P^{in} \rangle$ will also have some contribution around |t|=0, but it is much weaker, so it could be neglected. This means that if the first reflector has a sufficiently long distance from the noise sources, we can still select the needed components for use in the inversion scheme from the total crosscorrelation panel $\langle P^{\dagger}P \rangle$. In other words, instead of picking out the events explicitly in the data domain and then crosscorrelating the corresponding components, the separation can be made in the crosscorrelation panel of the total field for noise sources.

Example

To illustrate the workflow, we use a 2D model shown in Figure 2. 51 subsurface sources are distributed regularly along a synthetic drilling trajectory with an average spacing Δx=30m. 80 receivers are evenly placed with a spacing of Δ x=25m at the depth z=5m. The modelled acoustic pressure fields are computed with an elastic Finite Difference code without the free surface. In this example, although for the moment a Ricker wavelet of a central frequency of 15Hz is used, we expect the total crosscorrelation panel $\langle P^{\dagger}P \rangle$ to be similar for noise sources with the same source signature. Figure 3a shows an example of $\langle P^{\dagger}P \rangle$ for shot 25. We can see that $\langle P^{out\dagger}P^{out} \rangle$ and $\langle P^{out\dagger}P^{in} \rangle$ can be easily separated by applying a time window for |t|<0.7 and t>1.5, respectively. Figure 3b and 3c show the corresponding slice of $\langle P^{out\dagger}P^{out} \rangle$ an $\langle P^{out\dagger}P^{in} \rangle$. For verification, $\langle P^{in\dagger}P^{in} \rangle$ is computed separately and shown in Figure 3d. We see that it is indeed weak and therefore can be neglected.

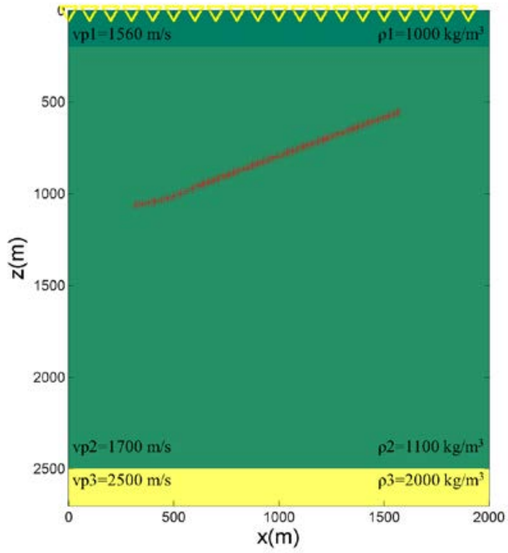

To compare, the reference response and the retrieved dipole Green's functions between the source positions are shown in Figure 4. The reference response, shown in blue, is the directly modelled vertical velocity field (with the direct arrivals removed for comparison) in a reference state where the medium above the source positions is homogenous. The direct arrivals are also removed in the virtual response obtained by CC, which is given by panel 3c. Overall we can see that the retrieved virtual response by MDD, obtained by deconvolving panel 3c by 3b, is satisfactory and has less spurious events.

Figure 2 *The P wave velocity model. The yellow triangles represent the receivers at the surface and the red stars represent the sources in the subsurface. All 51 sources and every fourth receiver of a total of 80 are plotted. The model has a grid spacing of 5 meter.*

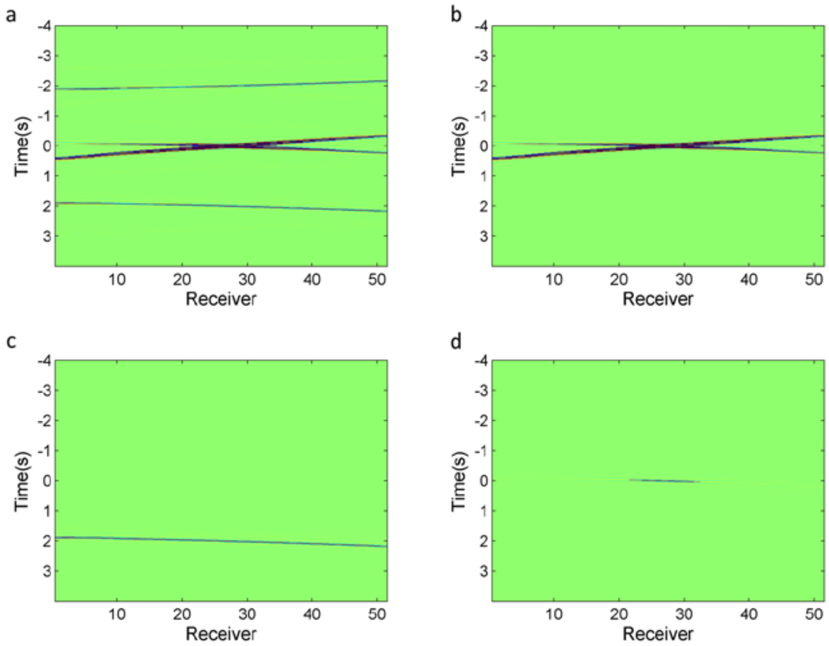

Figure 3 *Analysis of* $\langle P^{\dagger}P \rangle$

a) Slice of $\langle P^{\dagger}P \rangle$,

b) Slice of $\langle P^{out\dagger}P^{out} \rangle$,

c) Slice of $\langle P^{out\dagger}P^{in} \rangle$,

d) $\langle P^{in\dagger}P^{in} \rangle$. *All the images are plotted using the same color scale and correspond to the shot 25 at x=1250 m.*

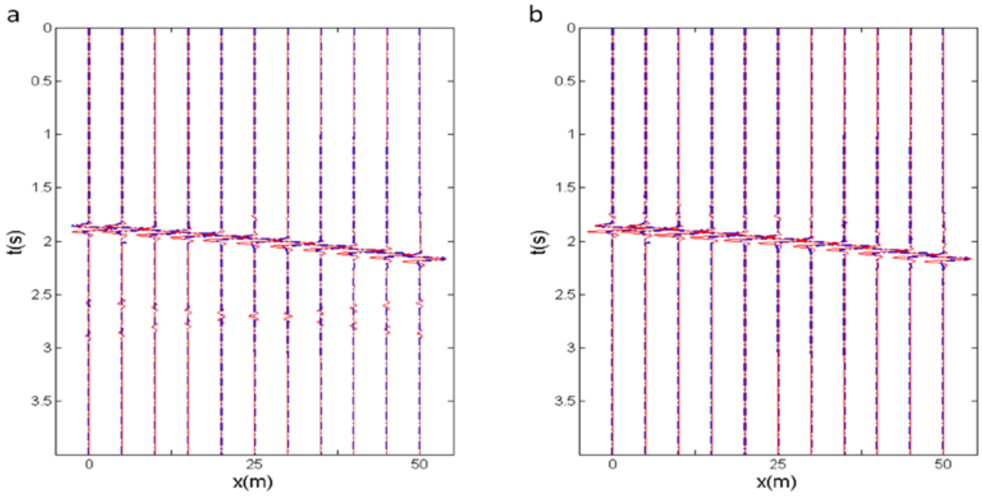

Figure 4 *Comparison of the retrieved response and the reference response. a) Retrieved response by CC (red) compared with the reference response (blue). Every fifth trace is plotted. b) Retrieved response by MDD (red) compared with the reference response (blue).*

Conclusions

By applying source and receiver reciprocity and following the method for non-transient uncorrelated noise sources as shown by Wapenaar and Fokkema (2006) and van der Neut (2010), we extend the method of inter-source SI (Curtis et al., 2009) to accommodate noise sources. We illustrate the workflow to separate the necessary ingredients for use in the inversion scheme, provided that the noise sources have the same source signature and the first reflector below the noise sources is relatively deep. With this separation in the intermediate crosscorrelation step, in theory one can turn the noise sources into virtual receivers in the subsurface. The result also shows that SI by MDD generates responses with less spurious events and removes the effect from the overburden.

Acknowledgements

This work is supported by the Deep Imaging and Geo-steering project of the Drilling and Well Centre for Improved Recovery (DrillWell) and the ROSE consortium at Norwegian University of Science and Technology. We thank Espen Birger Raknes for sharing the forward modelling code and Joost van der Neut and Deyan Draganov for discussions.

References

Curtis A., Nicolson H., Halliday D., Trampert J., and Baptie B., 2009. Virtual seismometers in the subsurface of the Earth from seismic interferometry. *Nature Geoscience*, **2**, 700 - 704.

Liu Y., Arntsen B., Wapenaar K. and Romdhane A., 2013. Inter-source seismic interferometry by multidimensional deconvolution (MDD) for borehole sources. *CPS/SEG 2014 Conference*

Menke W., 1989. Geophysical data analysis. *Academic Press*, San Diego, CA.

Van der Neut, J., Ruigrok R., Draganov D. and Wapenaar K., 2010. Retrieving the Earth's reflection response by multi-dimensional deconvolution of ambient seismic noise. *72nd EAGE Conference and Exhibition, Extended Abstracts*, P406.

Wapenaar K. and Fokkema J., 2006. Green's function representations for seismic interferometry. *Geophysics*, **71**, SI33-SI46.

Wapenaar K., van der Neut J., and Ruigrok E., 2008., Passive seismic interferometry by multi-dimensional deconvolution. *Geophysics*, **73**, A51- A56.

Wapenaar K., van der Neut J., Ruigrok E., Draganov D., Hunziker J., Slob E., Thorbecke J., and Snieder R., 2011. Seismic interferometry by crosscorrelation and by multidimensional deconvolution: a systematic comparison. *Geophysical Journal International*, **185**, 1335 - 1364.